



## Rainfall measurement using cell phone links: classification of wet and dry periods using geostationary satellites

T. I. van het Schip, A. Overeem , H. Leijnse, R. Uijlenhoet , J. F. Meirink & A. J. van Delden

To cite this article: T. I. van het Schip, A. Overeem , H. Leijnse, R. Uijlenhoet , J. F. Meirink & A. J. van Delden (2017) Rainfall measurement using cell phone links: classification of wet and dry periods using geostationary satellites, Hydrological Sciences Journal, 62:9, 1343-1353, DOI: [10.1080/02626667.2017.1329588](https://doi.org/10.1080/02626667.2017.1329588)

To link to this article: <http://dx.doi.org/10.1080/02626667.2017.1329588>



Published online: 05 Jun 2017.



Submit your article to this journal [↗](#)



Article views: 95



View related articles [↗](#)



View Crossmark data [↗](#)

## Rainfall measurement using cell phone links: classification of wet and dry periods using geostationary satellites

T. I. van het Schip<sup>a,b,\*</sup>, A. Overeem<sup>id a,c</sup>, H. Leijnse<sup>a</sup>, R. Uijlenhoet<sup>id c</sup>, J. F. Meirink<sup>a</sup> and A. J. van Delden<sup>b</sup>

<sup>a</sup>Royal Netherlands Meteorological Institute (KNMI), De Bilt, The Netherlands; <sup>b</sup>Institute for Marine and Atmospheric Research (IMAU), Utrecht University, Utrecht, The Netherlands; <sup>c</sup>Hydrology and Quantitative Water Management Group, Wageningen University, Wageningen, The Netherlands

### ABSTRACT

Commercial cellular telecommunication networks can be used for rainfall estimation by measuring the attenuation of electromagnetic signals transmitted between antennas from microwave links. However, as the received link signal may also decrease during dry periods, a method to separate wet and dry periods is required. Methods utilizing ground-based radar rainfall intensities or nearby link data cannot always be used. Geostationary satellites can provide a good alternative. A combination of two Meteosat Second Generation satellite precipitation products, Precipitating Clouds and Cloud Physical Properties, is employed to decide whether a 15-min time interval for a given link is rainy or not. A 12-d dataset of link-based rainfall maps for the Netherlands is validated against gauge-adjusted radar rainfall maps. Results clearly improve upon the case when no wet–dry classification is applied and thus the method shows potential for application to large areas of the world where the other methods cannot be applied.

### ARTICLE HISTORY

Received 7 July 2016  
Accepted 10 February 2017

### EDITOR

R. Woods

### ASSOCIATE EDITOR

G. Di Baldassarre

### KEYWORDS

observations; rainfall;  
microwave links; satellites

## 1 Introduction

Accurate rainfall measurements are very important for, e.g., numerical weather prediction model input, agriculture, water resource management, hydrology and climatology. Rainfall at regional scales is primarily measured using ground-based weather radars, satellites (such as the Global Precipitation Measurement mission or Meteosat Second Generation) and raingauges. Unfortunately, weather radar measurements are prone to errors, such as those caused by attenuation of the radar beam due to heavy rainfall, non-optimal conversion of radar reflectivity factors to rainfall intensities due to the variability of the drop size distribution, a non-uniform vertical profile of reflectivity, and overshooting of precipitation. For more details on these and other errors, see, for example, Joss and Waldvogel (1990), Doviak and Zrníć (1993), Michelson *et al.* (2005) or Fabry (2015). Hence, a common approach to measure precipitation is to adjust radar rainfall depths using raingauge rainfall depths. Raingauges can, if well maintained, provide accurate point measurements. However, the spatial resolution of a raingauge product is often low. In addition, the world coverage of radar and raingauges is limited mostly to Europe, North America and parts of South America, Asia and Australia. Particularly the

extent of the African observation network is very limited (Trans-African Hydro-Meteorological Observatory (TAHMO), 2017). Hence, other measurement techniques are needed to improve the spatial resolution of surface rainfall observations.

One promising technique is to employ microwave links from cellular telecommunication networks for rainfall estimation. Messer *et al.* (2006; for Israel) and Leijnse *et al.* (2007; for the Netherlands) were the first to show that these links can be used to measure rainfall. A microwave link consists of an antenna that transmits a microwave signal and a second antenna that receives the transmitted signal. The principal idea is that the signal transmitted from one antenna to the other is attenuated by rainfall. For the dataset from the Netherlands used here, the minimum and maximum received power of each 15-min period is stored by the cellular telecommunication company for monitoring the network stability. From the decrease in power compared to the dry weather signal level, the attenuation can be calculated, which in turn can be translated into a path-averaged rainfall depth (Atlas and Ulbrich 1977). Overeem *et al.* (2011) and Overeem *et al.* (2013) applied this method of measuring rainfall to, respectively, an urban area and the entire land surface of the

Netherlands, with promising results. Overeem *et al.* (2013) compared 12 daily link rainfall maps, based on ~2400 links, against a gauge-adjusted radar dataset, and found a squared correlation coefficient of 0.73, a coefficient of variation of 0.53 and a bias of almost zero. The potential of this new measurement technique has also been confirmed by, for instance, Chwala *et al.* (2012) for a mountainous region in Germany, by Doumounia *et al.* (2014) for Burkina Faso, Africa, by Hoedjes *et al.* (2014) for Kenya, Africa, and, again for the Netherlands, by Overeem *et al.* (2016b) employing a 2.5-year dataset of ~2000 link paths. Other studies are from the Czech Republic (Fencl *et al.* 2015), France (Schleiss *et al.* 2013) and Switzerland (e.g. Bianchi *et al.* 2013). Overeem *et al.* (2016b) evaluated the quality of link-based and gauge-based rainfall maps, and showed that the links perform equally well as raingauges for daily rainfall in summer, and even outperform raingauges for hourly rainfall in summer.

Gosset *et al.* (2016), and even the cellular telecommunication industry (Ericsson 2016, GSM Association 2016) have recognized the potential of this technique. Cellular networks have the benefit of covering large areas close to the ground and are of high density, especially in urban areas. Figure 1 shows the countries for which, to the best of our knowledge, researchers have managed to obtain commercial microwave link (CML) data. This has resulted in scientific papers for some of the countries shown, which are mentioned above.

The rainfall retrieval algorithm consists of the following steps (Overeem *et al.* 2013, 2016a, 2016b):

- (1) pre-processing of link data;
- (2) wet–dry classification using nearby links;
- (3) reference signal level determination;

- (4) removal of outliers;
- (5) correction of received signal powers;
- (6) computation of minimum and maximum rainfall intensities and conversion to mean path-averaged rainfall intensities.

Here we follow this approach, except that (2) is omitted, or performed employing radar or satellite data, and (4) is omitted. Overeem *et al.* (2016b) also developed and applied a filter to remove dew-induced wet antenna attenuation.

Decreases in the received link signal level can also occur during dry weather. This is associated with, e.g., absorption by atmospheric particles, dew on the antennas, receiver temperature variations and reflections. Such decreases should not be interpreted erroneously as being due to rainfall on the path between the transmitting and receiving antennas. Therefore, a method is needed to separate the rainy from the non-rainy periods. Moreover, in order to calculate the attenuation caused by rainfall, a reference level representing dry weather conditions has to be defined, which becomes more accurate if a wet–dry classification is performed. One way to classify wet and dry periods is to use weather radar (the “radar approach”, Overeem *et al.* 2011). According to this method, a 15-min period in which the mean 15-min path-averaged radar rainfall intensity exceeds  $0.1 \text{ mm h}^{-1}$  is classified as wet. The next 15-min time interval is also classified as wet, because it takes time for precipitation measured aloft by the radar to reach the Earth’s surface. A second method (the “link approach”; Overeem *et al.* 2011, 2013) uses the received powers of links located near the selected link. According to this method, a power decrease detected simultaneously by multiple links in

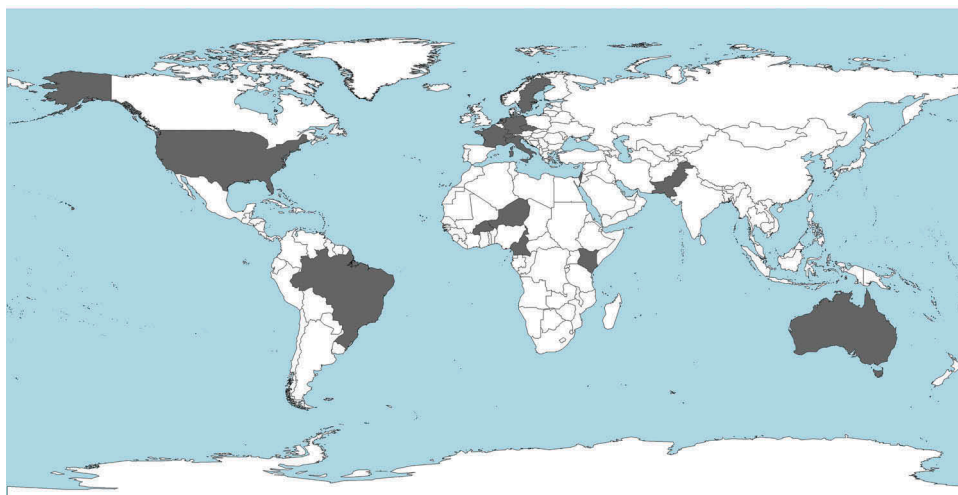


**Figure 1.** World map showing the countries for which researchers have managed to obtain CML data (shaded areas).

the vicinity of the selected link is interpreted as an indication that the detected loss of power over the selected link is due to rainfall. While the link and radar approaches show promising results, these methods cannot always be applied due to the unavailability of weather radar data and/or an insufficient number of nearby links. Other methods can be applied to received powers or signal attenuations when they are sampled at very high temporal frequencies, e.g. every 6 or 30 s (Schleiss and Berne 2010). For instance, Chwala *et al.* (2012) presented a spectral time series analysis, and Wang *et al.* (2012) Markov switching models.

Here, a novel method is presented to distinguish wet and dry periods for microwave link rainfall estimation. Geostationary satellites provide almost worldwide coverage at an acceptable temporal resolution of 15 min and could potentially be used to select wet and dry periods between roughly 70°N and 70°S. The objective of this paper is to develop a new wet–dry classification scheme using such satellite data. To facilitate an objective comparison, this is done for the same region (the Netherlands; ~50.5–53.5°N and ~3–7°W) and time period as was considered in Overeem *et al.* (2013). It is investigated whether application of this classification method would be useful, i.e. if it would provide better results than applying no wet-dry classification, when the existing link and radar approaches are not applicable.

Section 2 describes the microwave link, radar and satellite data; the methodology is explained in Section 3; the results are presented in Section 4; and, finally, conclusions and discussions are provided in Section 5.

## 2 Data

The 12-d calibration dataset and the 12-d validation dataset are identical to those used by Overeem *et al.* (2013). The calibration dataset consists of 12 days from June and July 2011. The validation dataset consists of 12 days from June, August and September 2011. The calibration and validation datasets are independent. The datasets contain both wet and dry periods. The link, radar and gauge-adjusted radar data used here are the same as described in Overeem *et al.* (2013).

### 2.1 Microwave link data

The minimum and maximum received signal level data were obtained from a CML network covering the Netherlands (having a surface area of about  $3.5 \times 10^4 \text{ km}^2$ ). The, on average, 2400 links from the validation dataset are located typically at some tens of metres above the ground, have frequencies between 13

and 40 GHz and an average path length of 3.1 km. Minimum and maximum received powers are available over 15-min intervals and are reported in integer dB values, based on 10 Hz sampling. The links have a single frequency and the majority transmit vertically polarized signals. The locations of the links are shown in Figure 2.

### 2.2 Radar data

The employed radar dataset was obtained from two C-band Doppler weather radars in the Netherlands, operated by the Royal Netherlands Meteorological Institute (KNMI). One is located in De Bilt, the other in Den Helder (shown in Fig. 2 by white circles). The data have a 5-min temporal and  $0.9\text{-km}^2$  spatial resolution. A detailed description of the radar data can be found in Overeem *et al.* (2009a, 2009b, 2011, 2013). The raingauge data used for the adjustment of the radar data were obtained from 325 daily manual and 32 hourly automatic raingauges. The data from the manual raingauges were collected daily at 0800 UTC. The gauge-adjusted radar dataset is freely available at the Climate4Impact website (<http://climate4impact.eu>; “Radar precipitation climatology”).

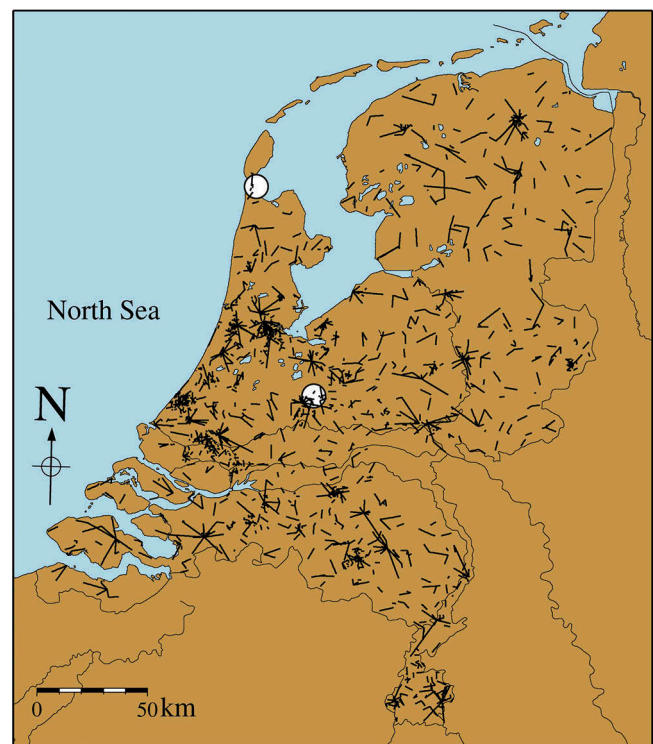


**Figure 2.** Map of the Netherlands with the locations of the CML paths for the validation used in this paper. The white circles show the locations of the radars.

### 2.3 Satellite data

The land surface area of the Netherlands is covered by the Meteosat Second Generation (MSG) satellite, carrying the Spinning Enhanced Visible and InfraRed Imager (SEVIRI) instrument, which takes images of the Earth every 15 min. Its spatial resolution is approximately  $4 \times 7 \text{ km}^2$  for the Netherlands. Various precipitation products exist that are based on SEVIRI measurements. The EUMETSAT Nowcasting and Very Short Range Forecasting Satellite Application Facility (NWC SAF) provides, for instance, the Precipitating Clouds (PC) product (corrected for parallax). PC gives a precipitation likelihood for intensities larger than  $0.1 \text{ mm h}^{-1}$ . The likelihood ranges from 0 to 100% with intervals of 10%. In addition, the Cloud Physical Properties (CPP) product is employed (Roebeling and Holleman 2009; freely available at <https://data.knmi.nl/>). It gives a precipitation rate in  $\text{mm h}^{-1}$ . CPP relies on the retrieval of cloud optical and microphysical properties, which requires visible/near-infrared reflectance as input. Therefore, CPP is only available during the daytime. Note that a parallax correction has been applied here. More information on both products can be found at <http://www.nwcsaf.org/>.

## 3 Methods

### 3.1 Rainfall retrieval from link data

When rain is present along the path between the transmitter and receiver the signal is attenuated, as raindrops scatter some of the energy out of the beam and absorb another part of the signal, leaving less energy to be received than in the absence of rainfall. The attenuation becomes larger for increasing numbers and sizes of raindrops. By measuring the received power as a function of time, the attenuation due to rainfall can be determined and the path-averaged rainfall over the link can be calculated from the decrease in signal power (Overeem *et al.* 2011).

One source of error in the calculation of rainfall intensities is the presence of decreased signal levels not related to rainfall. It is crucial to have good information about wet and dry periods, as signal attenuation during dry weather can lead to non-zero microwave link rainfall estimates. This also facilitates robust estimation of the reference level of the received power signal,  $P_{\text{ref}}$ .

Two methods for wet–dry classification have already been developed and are called the “link approach” and the “radar approach” (Overeem *et al.* 2011). When the link approach is used, a 15-min interval is labelled wet if the mutual decrease in minimum received powers

$P_{\text{min}}$  of nearby links within a 15-km radius exceeds two threshold values for that interval (Overeem *et al.* 2013, 2016a). These thresholds have been obtained from Overeem *et al.* (2011), where they were optimized using link data from another network and period. This approach makes use of the fact that rain events have a certain spatial correlation (Van de Beek *et al.* 2012). When rainfall occurs in a given 15-min interval, multiple links in the vicinity are likely to be affected rather than just one (assuming that the links are located less than 15 km apart).

The radar approach uses unadjusted radar data from the weather radars located in De Bilt and Den Helder (see Fig. 2). If the radar measures a path-averaged rainfall intensity larger than  $0.1 \text{ mm h}^{-1}$  (i.e. 7 dBZ) for a 15-min interval, the current and next time interval are assumed wet to account for a typical delay of 3–12 min between rain measured by radar generally at 1.5 km altitude for this product and that measured at the Earth’s surface.

After classifying the wet and dry periods, the reference signal level  $P_{\text{ref}}$  is determined for each link and each 15-min interval. For each 15-min interval the minimum and maximum received powers  $P_{\text{min}}$  and  $P_{\text{max}}$  are stored by the network provider. The average of these two numbers,  $\bar{P}$ , is obtained for each link and for each time interval. The reference level for a time interval is found by taking the median of the  $\bar{P}$  values of those time intervals from the preceding 24 hours which are classified as dry. The median is taken to limit the influence of outliers. The reference level, and therefore the rain intensity, is not calculated on the rare occasions when fewer than 10 dry periods of 15 min (i.e. less than 2.5 h) are detected in the previous 24 h.

The reference level is used to remove decreases in signal power not related to rainfall and to calculate the path-averaged rainfall intensity  $\langle R \rangle$  from minimum and maximum path-averaged specific attenuation,  $\langle k_{\text{min}} \rangle$  and  $\langle k_{\text{max}} \rangle$  (Overeem *et al.* 2011). Before calculating the path-averaged rainfall intensity  $\langle R \rangle$  from  $\langle k_{\text{min}} \rangle$  and  $\langle k_{\text{max}} \rangle$ , Overeem *et al.* (2013) applied a filter to remove local outliers caused by malfunctioning links. This outlier filter depends on the link approach. The aim of this paper is to study the performance of the wet–dry classification using satellite data compared to (1) applying no wet–dry classification at all and (2) the wet–dry classification using radar data (the reference). Hence, these approaches should be independent from the link approach, and therefore the outlier filter will not be applied. Note that if no wet–dry classification has been applied, the reference level is determined as the median

of the  $\bar{P}$  values over all time intervals in the previous 24 h.

Further details concerning the retrieval method can be found in Overeem *et al.* (2016a). They give an extensive description of the rainfall retrieval algorithm and accompanying code, including no wet–dry classification. They also provide sensitivity analyses of parameters of the rainfall retrieval algorithm. In addition, they supply a working example, including one day of the validation dataset used here. The code and the example dataset is freely available at GitHub (<https://github.com/overeem11/RAINLINK>).

### 3.2 Satellite approach

#### 3.2.1 Selection of satellite products

Since the CPP product is only available during daylight, the PC and CPP products were combined with the goal of wet–dry classification in link rainfall retrievals, i.e. the “satellite approach”. Note that during the night only the PC product is used. A pixel is considered wet if one or both of the satellite products indicates rain: the pixel should have a precipitation probability of at least 20% according to the PC product or a rainfall intensity of at least  $0.1 \text{ mm h}^{-1}$  according to the CPP product. The decision to classify a pixel as wet when at least one of the satellite products detects rain, rather than using the condition that both products should detect rain, is made because for this application it is important for the wet–dry classification not to miss a wet area and therefore not to incorrectly classify a pixel as dry (i.e. a false negative).

#### 3.2.2 Wet–dry classification

The combined PC and CPP product is now employed for wet–dry classification in the algorithm to estimate rainfall using microwave links. Light precipitation at the edge of a cloud is easily missed by satellites (Amorati *et al.* 2000). The rainfall area detected by the satellite is therefore systematically extended by one satellite pixel in all directions for the PC and CPP product when used in the wet–dry classification.

An interval is classified as dry if neither product detects rain over the link path, otherwise it is classified as wet. Time periods that are incorrectly classified as wet will often still become dry (i.e.  $R = 0 \text{ mm h}^{-1}$ ) when the PC and CPP products are used in the microwave link rainfall estimation, because a microwave link will mostly report no rain in the case of dry weather. A time period incorrectly classified as dry will always yield zero rainfall. Next, for each link the reference level of received signal powers is calculated using all

15-min time intervals that are classified as dry according to the PC and CPP products.

Figure 3 illustrates the wet–dry classification with the satellite approach for one day and one link. Minimum received powers decline in case of rain, i.e. for non-zero path-averaged radar rainfall intensities. Around 0400 UTC minimum received powers show a gradual decline. The lower received powers last around 5 hours, whereas no rain is observed along the link path by the merged radar-gauge rainfall product. The satellite approach successfully classifies this period as dry, resulting in non-declining corrected received powers.

### 3.3 Calibration and validation methodology

To optimize two coefficients of the rainfall retrieval algorithm, link data from the calibration dataset are compared to gauge-adjusted radar data, assumed to be the ground truth, i.e. the reference. The residual is the difference between the link-based daily rainfall depth and the gauge-adjusted radar daily rainfall depth over a link path. Optimal values of  $A_a$  (the attenuation due to wet antennas in dB) and  $\alpha$  (a coefficient determining the contribution of the minimum and maximum to the mean rainfall intensity during a 15-min time interval) are obtained for the 12-d calibration dataset by minimizing the residual standard deviation subject to the condition that the absolute value of the mean bias in daily accumulations is smaller than 0.02 mm. Using the optimal values of  $A_a$  and  $\alpha$ , the mean 15-min rainfall

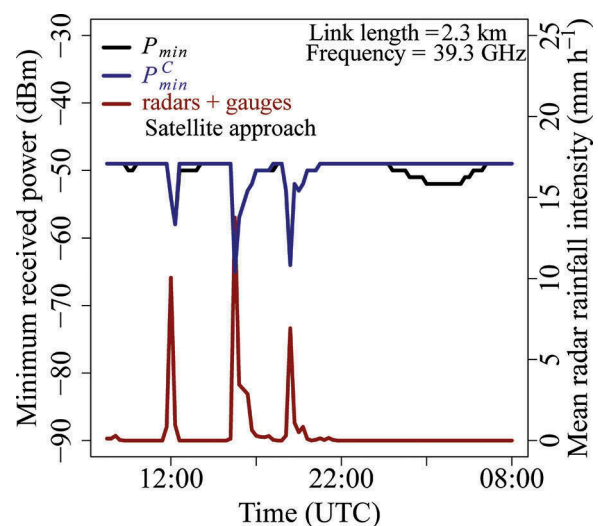


**Figure 3.** Minimum received power ( $P_{\min}$ ; black), corrected minimum received power ( $P_{\min}^C$ ; blue), and mean gauge-adjusted radar rainfall intensity (red) for one microwave link for 15-min intervals from 10 June 2011, 08:00 UTC to 11 June 2011, 08:00 UTC.

intensities are calculated for each time interval and for each link of the validation link dataset.

The radar approach is expected to perform the best wet–dry classification and is considered as the reference. Hence, it is most suitable to obtain optimal values of  $A_a$  and  $\alpha$  for the radar approach only. These values are also used when no wet–dry classification is applied and for the satellite approach. This ensures a fair comparison amongst approaches, i.e. differences will not be caused by different values of  $A_a$  and  $\alpha$ . Moreover, in this way these values are not much influenced by erroneous wet–dry classifications, since the radar approach is expected to perform quite well. Note also that the same attenuation–rain rate relationship parameters have been utilized for each approach. All datasets start with the same set of links, i.e. having the same microwave frequencies. The parameter values mainly depend on link frequency (Olsen *et al.* 1978; Overeem *et al.* 2016a, 2016b).

The optimized values,  $A_a = 2.55$  dB and  $\alpha = 0.305$ , are used to calculate rainfall intensities for the 12-d validation dataset. After the rainfall intensities have been calculated for the different links, the data are interpolated using ordinary kriging in order to create 15-min rainfall maps for the total land surface area of the Netherlands (Overeem *et al.* 2013, 2016a).

Daily rainfall maps are obtained for each day of the validation dataset by accumulating all 15-min rainfall maps. In order to quantify the performance of a given approach, scatter density plots with respect to the ground truth are constructed for the 15-min and daily rainfall maps with spatial resolutions of  $74 \text{ km}^2$  and  $0.9 \text{ km}^2$ , respectively. By using the mean rainfall depth over an area of  $74 \text{ km}^2$ , representativeness errors between radar and link rainfall depths are partly compensated. Furthermore, the mean radar and link rainfall depths, the coefficient of variation CV and the coefficient of determination  $\rho^2$  (the squared Pearson correlation coefficient) are calculated. The CV is the

ratio of the standard deviation of the residuals and the mean of the reference. Both the mean radar and link rainfall depths are calculated. For the scatter density plots, only those radar-link pairs are used where links, or radars, or both have measured at least 0.1 mm.

## 4 Results

The rainfall retrieval algorithm is applied to the 12 days of the validation dataset. The performance for three approaches is presented in the order: no wet–dry classification, the satellite approach, and the radar approach. In this manner it will be easy to see whether the satellite approach improves upon applying no wet–dry classification, and to what extent it meets the performance of the radar approach, considered as the best wet–dry classification method. Note that the temporal and spatial resolutions of the verified rainfall maps are rather high. Results will generally improve when lower resolutions are investigated.

Figures 4 and 5 show scatter density plots for 15-min rainfall maps with a resolution of  $74 \text{ km}^2$  and daily rainfall maps with a resolution of  $0.9 \text{ km}^2$ . The values of CV,  $\rho^2$ , the average rainfall depth measured using radars, indicated by  $\bar{R}_{\text{radar}}$ , and the average rainfall depth measured using links, indicated by  $\bar{R}_{\text{link}}$ , are included in the plots. An overview of these metrics is given in Tables 1 and 2.

$\bar{R}_{\text{radar}}$  and  $\bar{R}_{\text{link}}$  are calculated from those rainfall depths where links, or radars, or both have measured more than 0.1 mm. This is also the cause of the differences in  $\bar{R}_{\text{radar}}$  for the different approaches. All approaches, except for no wet–dry classification, show a slight underestimation of the mean 15-min and daily rainfall depths. The difference in performance between the various approaches can be seen best in CV and  $\rho^2$ .

Considering the 15-min link rainfall maps, the satellite approach gives a moderate improvement on the

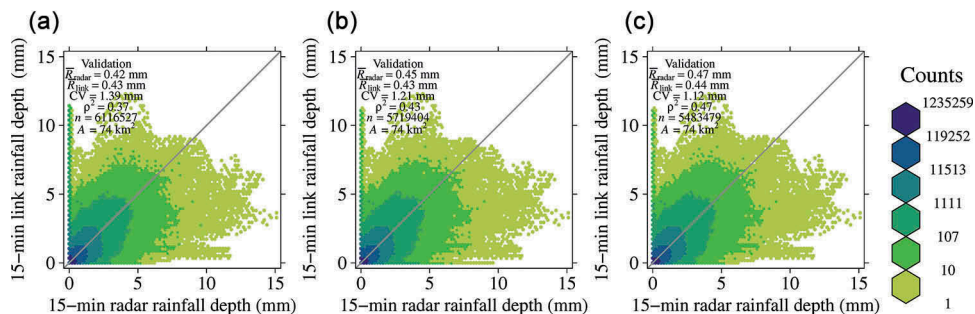


**Figure 4.** Validation of 15-min link rainfall maps against gauge-adjusted radar rainfall maps for an area  $A$  of  $74 \text{ km}^2$ .  $\bar{R}$  denotes the average rainfall depth, CV is the coefficient of variation and  $\rho^2$  is the coefficient of determination. Only those rainfall depths are used where links, or radars, or both have measured more than 0.1 mm. Validation of link rainfall maps using (a) no wet–dry classification, (b) the satellite approach, and (c) the radar approach.

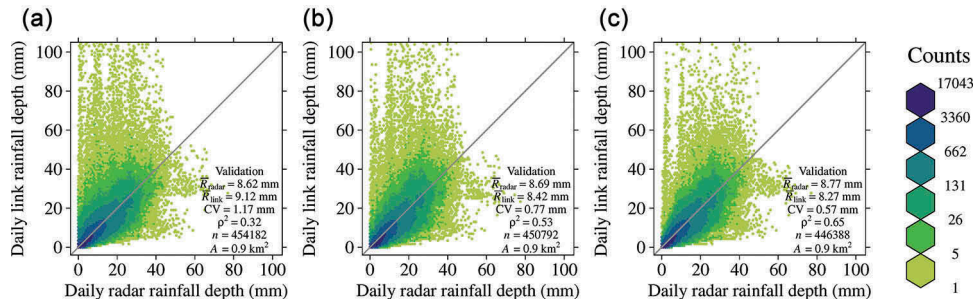


**Figure 5.** Validation of daily link rainfall maps against gauge-adjusted radar rainfall maps for an area  $A$  of  $0.9 \text{ km}^2$ . Validation of link rainfall maps using (a) no wet–dry classification, (b) the satellite approach, and (c) the radar approach. See Figure 4 caption for more information.

**Table 1.** Statistics of the 15-min link rainfall map validation for an area size of  $74 \text{ km}^2$  (i.e. the values of the coefficient of variation CV, the coefficient of determination  $\rho^2$ ,  $\bar{R}_{\text{radar}}$  and  $\bar{R}_{\text{link}}$ ).

	CV	$\rho^2$	$\bar{R}_{\text{radar}}$	$\bar{R}_{\text{link}}$
No wet–dry classification	1.39	0.37	0.42	0.43
Satellite approach	1.21	0.43	0.45	0.43
Radar approach	1.12	0.47	0.47	0.44

**Table 2.** Statistics of the daily link rainfall map validation for each radar pixel of  $0.9 \text{ km}^2$  (i.e. the values of the coefficient of variation CV, the coefficient of determination  $\rho^2$ ,  $\bar{R}_{\text{radar}}$  and  $\bar{R}_{\text{link}}$ ).

	CV	$\rho^2$	$\bar{R}_{\text{radar}}$	$\bar{R}_{\text{link}}$
No wet–dry classification	1.17	0.32	8.62	9.12
Satellite approach	0.77	0.53	8.69	8.42
Radar approach	0.57	0.65	8.77	8.27

case where no wet–dry classification is applied, as shown by the lower CV and slightly higher  $\rho^2$ . Only slightly better values are found for the radar approach,

confirming the quality of the satellite approach. Although Figure 4 demonstrates the ability of links to detect rain, even for the radar approach CV and  $\rho^2$  remain fairly high and low, respectively. This is partly related to representativeness errors in time and space between link measurements near the Earth’s surface and radar measurements aloft. Figure 6(a) shows a histogram of link rainfall depths above 2 mm for which the corresponding radar rainfall depth is below 0.5 mm. The satellite approach leads to a reasonable reduction in the number of extreme rainfall overestimations by links compared to applying no wet–dry classification.

Considering the daily rainfall depths, the satellite approach is clearly better than applying no wet–dry classification, as seen from a much lower CV and a much higher  $\rho^2$  value. The average bias in the mean of +6% for no wet–dry classification changes to –3% for the satellite approach. A group of large overestimations is removed (compare the upper-left corners of panels

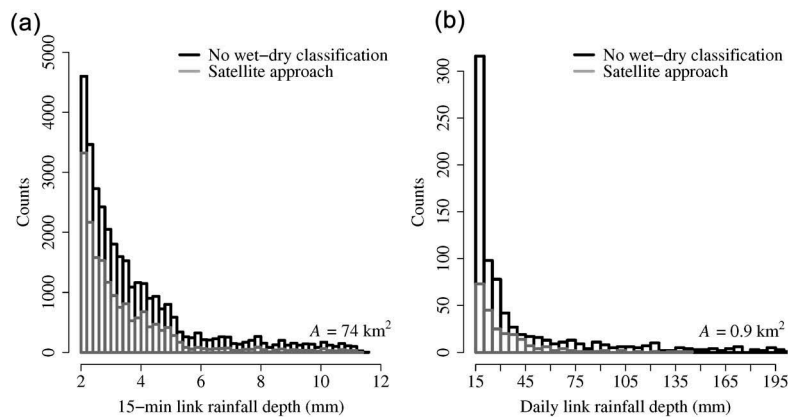


**Figure 6.** Counts of link rainfall depths for a range of rainfall classes for (a) 15-min and (b) daily rainfall maps from the 12-d validation dataset. First, only those radar–link pairs are selected where links, or radars, or both have measured at least 0.1 mm (the same selection as for Figs. 4 and 5). Next, only those link rainfall depths are counted for which the corresponding radar rainfall depth is below the threshold value given in the figure title. In order to study severe overestimation by links with respect to radar, counts are only presented for link rainfall depths much higher than the chosen threshold, i.e. those larger than or equal to (a) 2 mm or (b) 15 mm.



(a) and (b)). This is investigated in more detail in [Figure 6\(b\)](#) for link rainfall depths above 15 mm for which the corresponding radar rainfall depth is below 2 mm. The high daily link rainfall values may, for instance, be caused by dew formation on antennas or by malfunctioning links. The satellite approach leads to a large reduction in the number of extreme rainfall overestimations by links compared to applying no wet–dry classification.

The radar approach performs even better than the satellite approach, except for the bias in the mean, which becomes 6%. Note that it uses unadjusted radar data and therefore partly depends on the reference rainfall dataset of gauge-adjusted radar data. The satellite approach is a useful method compared to the case where no wet–dry classification is applied. Hence, the geostationary satellite approach could be an effective wet–dry classification method for regions all around the world with an insufficient number of links and/or no radar data.

To illustrate the ability of microwave links in cellular telecommunication networks to detect rainfall patterns, four out of twelve daily rainfall maps from the validation dataset are presented in [Figure 7](#). The first column shows the daily rainfall depth determined from cell phone links without correcting for decreases in signal level that are not related to rainfall. The second column displays the results for the satellite approach. The third column reveals the results for the radar approach. The last column shows the gauge-adjusted radar rainfall maps, which are considered to be the ground truth.

[Figure 7](#) shows that the rainfall patterns detected by the radars are to a large extent also detected by the links for all approaches, with comparable rainfall depths. The large outlier seen when no wet–dry classification is applied on 11 June 2011 (first row) is strongly reduced when the satellite approach is used. The outlier seen on 9 August 2011 (second row), is completely removed when using the satellite approach. Not all outliers are removed when the satellite

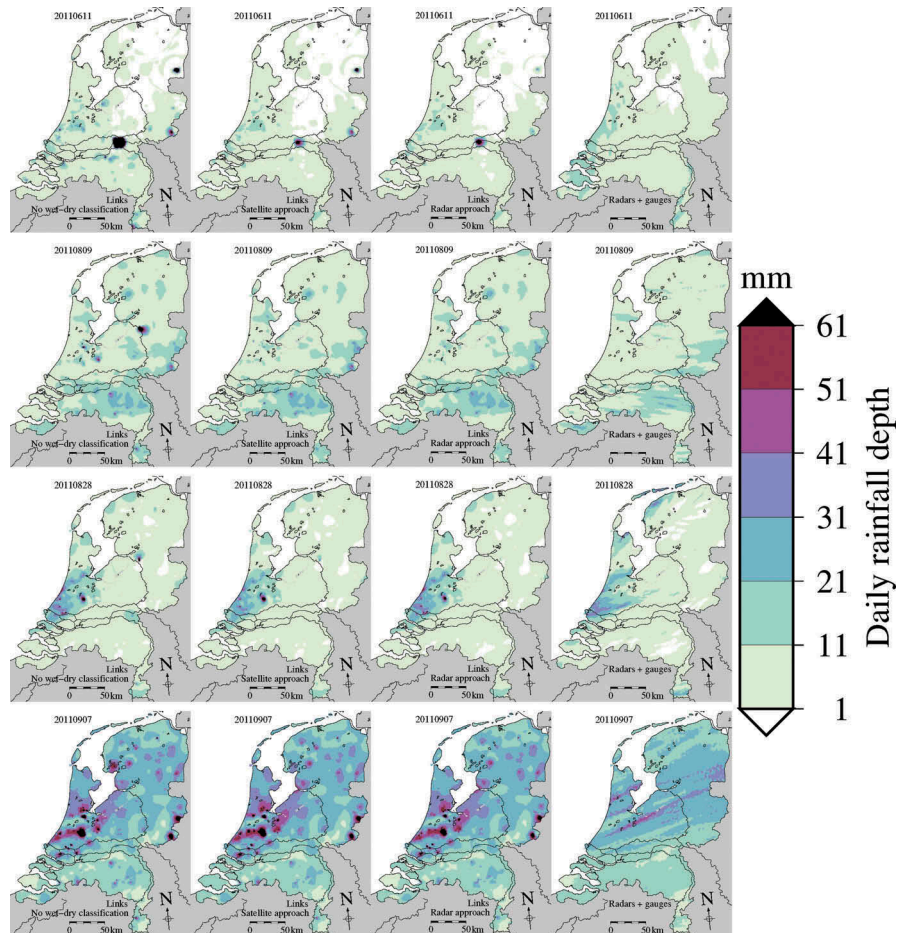


**Figure 7.** Daily rainfall maps for four days (ending at 08:00 UTC) of the validation dataset of 12 days for, from left to right: links, no wet–dry classification; links, wet–dry classification with PC + CPP satellite products (satellite approach); links, wet–dry classification using radar data (radar approach); and gauge-adjusted radar data (ground truth).

approach is applied, not even when the radar approach is employed (first, third and fourth rows). In general, differences between approaches are small given the rainfall classes used.

## 5 Conclusions and discussions

A new wet–dry classification method was developed for rainfall monitoring employing commercial cellular telecommunication networks. A combination of two geostationary precipitation products from the Meteosat Second Generation satellite, PC and CPP, was selected to classify wet and dry periods in the link rainfall retrieval algorithm. Although the satellite approach gave a clear improvement compared to the case with no wet–dry classification for 15-min rainfall maps, the benefit of a wet–dry classification using the satellite approach was found to be most pronounced for daily rainfall.

This new wet–dry classification method could be a valuable alternative for areas around the world where no weather radars are available and the link network is not dense enough to apply the link approach, e.g. large parts of South America, Africa and Asia. Note that geostationary satellites have a much larger areal coverage than radars and raingauges (Heistermann *et al.* 2013). A combined satellite–link rainfall product holds promise for providing better rainfall estimates compared to a satellite-only rainfall product. One of the reasons is that microwave links, in contrast to satellites, measure near the Earth's surface.

The use of the satellite approach to classify wet and dry periods gives clear improvements in the estimation of rainfall employing a commercial cellular telecommunication network over applying no wet–dry classification at all. However, when available, the radar approach is preferred, as its performance is better than the satellite approach. Results for the link approach (CV of 0.60,  $\rho^2$  of 0.64, bias in the mean of  $-7\%$ ), not shown in this study, are almost identical to those for the radar approach. Even better would be to use the link approach with a filter to remove malfunctioning links, as applied in Overeem *et al.* (2013), which particularly improves daily rainfall estimates (CV of 0.49,  $\rho^2$  of 0.72), except for the bias in the mean, which becomes  $-11\%$ . The results for the link approach discussed here have been obtained utilizing the same values of  $A_a$  (2.55 dB) and  $\alpha$  (0.305) as for the radar approach. Note that these values are quite close to those obtained for the link approach with outlier filter in Overeem *et al.* (2013): 2.30 dB for  $A_a$  and 0.33 for  $\alpha$ .

Since the parameter values in the rainfall retrieval algorithm are calibrated to the Dutch climate, their values could differ for other countries and networks. This holds, for instance, for  $A_a$  and  $\alpha$ . An extensive discussion of the rainfall retrieval algorithm is given in Overeem *et al.* (2016a), including prospects for use of this algorithm in other climates and for other link networks, e.g. in terms of sampling strategy.

The satellite approach has been tested for the Dutch climate. The validation over 12 rainy days, containing a large number of microwave links, shows that satellite products can be valuable for wet–dry classification as part of a link rainfall retrieval algorithm. It is recognized that the satellite products employed here may give different results for other climates. In the case of worse results, the satellite approach presented here may still be applied, however, by employing alternative satellite products, which are more appropriate for wet–dry classification in those climates. For instance, the MSG Convective Rainfall Rate (CRR) product may perform better for the African continent.

Rios Gaona *et al.* (2015) employed the same 12-d dataset as used here to study uncertainties in rainfall maps due to link rainfall retrieval errors and those related to the interpolation methodology, including spatial density of the network. The latter plays a minor, but non-negligible role in explaining differences between link and radar rainfall maps, particularly at short time scales (Fig. 4). For instance, radar provides full coverage over the Netherlands (around 38 000 pixels of  $0.9 \text{ km}^2$ ), whereas the number of links is approximately 2400. Moreover, other interpolation methodologies may be more appropriate, for instance, for climates with different spatial rainfall properties.

Although the radar approach is used as a reference, it also suffers from its own representativeness errors. As the radars measure precipitation aloft, instead of at the ground, it is possible that a time interval is incorrectly defined as wet. If the link measures attenuation during dry weather, this will lead to an overestimation of rainfall in such a case. The same reasoning holds for the satellite approach. Also note that the spatial resolution of the satellite products,  $\sim 4 \times 7 \text{ km}^2$ , is relatively coarse compared to the average link path length of 3.1 km.

Many satellite precipitation products are available (see e.g. Kidd and Huffman 2011, Ashouri *et al.* 2015), such as the IMERG product of the new Global Precipitation Measurement mission (Hou *et al.* 2014, Rios Gaona *et al.* 2016). Other satellite products may produce a better wet–dry classification than the MSG precipitation products. An advantage of the employed geostationary products is that they provide real-time

15-min data over vast areas, including Africa and Europe, which will generally not be achieved by products based on data from lower orbiting satellites (at best 30 min after interpolation). Despite the MSG precipitation products perhaps being suboptimal, they already provide a useful wet–dry classification for the Netherlands. This is interesting for Africa, which contains many (nearly) ungauged regions, which often have a cellular telecommunication infrastructure. Though it is generally not easy to gain access to microwave link data, researchers have managed to obtain data from, to the best of our knowledge, four African countries. Up to now this has resulted in studies based on data from Burkina Faso (Doumounia *et al.* 2014) and Kenya (Hoedjes *et al.* 2014), which is encouraging.

To conclude, the geostationary satellite approach for wet–dry classification in rainfall retrieval from cellular telecommunication networks is potentially widely applicable and promising.

## Acknowledgments

We would like to thank Ralph Koppelaar and Ronald Kloeg from T-Mobile NL for providing us with the microwave link data.

## Disclosure statement

No potential conflict of interest was reported by the authors.

## Funding

This work was supported by the Netherlands Technology Foundation STW (currently NWO Domain Applied and Engineering Sciences) under Grant 11944.

## ORCID

A. Overeem  <http://orcid.org/0000-0001-5550-8141>  
R. Uijlenhoet  <http://orcid.org/0000-0001-7418-4445>

## References

- Amorati, R., *et al.*, 2000. IR-based satellite and radar rainfall estimates of convective storms over northern Italy. *Meteorological Applications*, 7, 1–18. doi:10.1017/S1350482700001328
- Ashouri, H., *et al.*, 2015. PERSIANN-CDR: daily precipitation climate data record from multisatellite observations for hydrological and climate studies. *Bulletin of the American Meteorological Society*, 96, 69–83. doi:10.1175/BAMS-D-13-00068.1
- Atlas, D. and Ulbrich, C.W., 1977. Path- and area-integrated rainfall measurement by microwave attenuation in the 1–3 cm band. *Journal of Applied Meteorology*, 16, 1322–1331. doi:10.1175/1520-0450(1977)016<1322:PAIRM>2.0.CO;2
- Bianchi, B., Rieckermann, J., and Berne, A., 2013. Quality control of rain gauge measurements using telecommunication microwave links. *Journal of Hydrology*, 492, 15–23. doi:10.1016/j.jhydrol.2013.03.042
- Chwala, C., *et al.*, 2012. Precipitation observation using microwave backhaul links in the alpine and pre-alpine region of Southern Germany. *Hydrology and Earth System Sciences*, 16, 2647–2661. doi:10.5194/hess-16-2647-2012
- Doumounia, A., *et al.*, 2014. Rainfall monitoring based on microwave links from cellular telecommunication networks: first results from a West African test bed. *Geophysical Research Letters*, 41, 6016–6022. doi:10.1002/2014GL060724
- Doviak, R.J. and Zrnić, D.S., 1993. *Doppler radar and weather observations*. 2nd ed. San Diego: Academic Press. 562.
- Ericsson. 2016. Ericsson mobility report – on the pulse of the networked society. Available from: <https://www.ericsson.com/res/docs/2016/ericsson-mobility-report-2016.pdf> [Accessed 26 April 2017].
- Fabry, F., 2015. *Radar meteorology: principles and practice*. Cambridge, UK: Cambridge University Press.
- Fencl, M., *et al.*, 2015. Commercial microwave links instead of rain gauges: fiction or reality? *Water Science & Technology*, 71, 31–37. doi:10.2166/wst.2014.466
- Gosset, M., *et al.*, 2016. Improving rainfall measurement in gauge poor regions thanks to mobile telecommunication networks. *Bulletin of the American Meteorological Society*, 97, ES49–ES51. doi:10.1175/BAMS-D-15-00164.1
- GSM Association. 2016. mAgri: weather forecasting and monitoring: mobile solutions for climate resilience. Available from: <http://www.gsma.com/mobilefordevelopment/wp-content/uploads/2016/02/Weather-forecasting-and-monitoring-mobile-solutions-for-climate-resilience.pdf> [Accessed 26 April 2017].
- Heistermann, M., Jacobi, S., and Pfaff, T., 2013. Technical note: an open source library for processing weather radar data (wradlib). *Hydrology and Earth System Sciences*, 17, 863–871. doi:10.5194/hess-17-863-2013
- Hoedjes, J.C.B., *et al.*, 2014. A conceptual flash flood early warning system for Africa, based on terrestrial microwave links and flash flood guidance. *ISPRS International Journal of Geo-Information*, 3, 584–598. doi:10.3390/ijgi3020584
- Hou, A.Y., *et al.*, 2014. The global precipitation measurement mission. *Bulletin of the American Meteorological Society*, 95, 701–722. doi:10.1175/BAMS-D-13-00164.1
- Joss, J. and Waldvogel, A., 1990. Precipitation measurement and hydrology. In: L.J. Battan and D. Atlas, eds. *Radar in meteorology*. Boston, MA: American Meteorological Society, 577–606.
- Kidd, C. and Huffman, G., 2011. Global precipitation measurement. *Meteorological Applications*, 18, 334–353. doi:10.1002/met.284
- Leijnse, H., Uijlenhoet, R., and Stricker, J.N.M., 2007. Rainfall measurement using radio links from cellular communication networks. *Water Resources Research*, 43, 1–6. doi:10.1029/2006WR005631
- Messer, H., Zinevich, A., and Alpert, P., 2006. Environmental monitoring by wireless communication networks. *Science*, 312, 713. doi:10.1126/science.1120034
- Michelson, D.B., *et al.*, 2005. COST action 717. *Use of radar observation in hydrological and NWP models. Weather radar data quality in Europe: quality control and*

- characterisation – review*. Luxembourg: EU Publications Office (EUR 21955), 87.
- Olsen, R.L., Rogers, D.V., and Hodge, D.B., 1978. The  $aR^b$  relation in the calculation of rain attenuation. *IEEE Transactions on Antennas and Propagation*, 26, 318–329. doi:10.1109/TAP.1978.1141845
- Overeem, A., Buishand, T.A., and Holleman, I., 2009a. Extreme rainfall analysis and estimation of depth-duration-frequency curves using weather radar. *Water Resources Research*, 45, 1–15. doi:10.1029/2009WR007869
- Overeem, A., Holleman, I., and Buishand, T.A., 2009b. Derivation of a 10-year radar-based climatology of rainfall. *Journal of Applied Meteorology and Climatology*, 48, 1448–1463. doi:10.1175/2009JAMC1954.1
- Overeem, A., Leijnse, H., and Uijlenhoet, R., 2011. Measuring urban rainfall using microwave links from commercial cellular communication networks. *Water Resources Research*, 47, 1–16. doi:10.1029/2010WR010350
- Overeem, A., Leijnse, H., and Uijlenhoet, R., 2013. Country-wide rainfall maps from cellular communication networks. *Proceedings of the National Academy of Sciences of the United States of America*, 110, 2741–2745. doi:10.1073/pnas.1217961110
- Overeem, A., Leijnse, H., and Uijlenhoet, R., 2016a. Retrieval algorithm for rainfall mapping from microwave links in a cellular communication network. *Atmospheric Measurement Techniques*, 9, 2425–2444. doi:10.5194/amt-9-2425-2016
- Overeem, A., Leijnse, H., and Uijlenhoet, R., 2016b. Two and a half years of country-wide rainfall maps using radio links from commercial cellular telecommunication networks. *Water Resources Research*, 52, 8039–8065. doi:10.1002/2016WR019412
- Rios Gaona, M.F., *et al.*, 2015. Measurement and interpolation uncertainties in rainfall maps from cellular communication networks. *Hydrology and Earth System Sciences*, 19, 3571–3584. doi:10.5194/hess-19-3571-2015
- Rios Gaona, M.F., *et al.*, 2016. First-year evaluation of GPM-rainfall over the Netherlands: IMERG day-1 final run (V03D). *Journal of Hydrometeorology*, 17, 2799–2814. doi:10.1175/JHM-D-16-0087.1
- Roebeling, R.A. and Holleman, I., 2009. SEVIRI rainfall retrieval and validation using weather radar observations. *Journal of Geophysical Research: Atmospheres*, 114, 1–13. doi:10.1029/2009JD012102
- Schleiss, M. and Berne, A., 2010. Identification of dry and rainy periods using telecommunication microwave links. *IEEE Geoscience and Remote Sensing Letters*, 7, 611–615. doi:10.1109/LGRS.2010.2043052
- Schleiss, M., Rieckermann, J., and Berne, A., 2013. Quantification and modeling of wet-antenna attenuation for commercial microwave links. *IEEE Geoscience and Remote Sensing Letters*, 10, 1195–1199. doi:10.1109/LGRS.2012.2236074
- Trans-African Hydro-Meteorological Observatory (TAHMO), 2017. Available from: [www.tahmo.org/](http://www.tahmo.org/) [Accessed 26 April 2017].
- Van de Beek, C.Z., *et al.*, 2012. Seasonal semi-variance of Dutch rainfall at hourly to daily scales. *Advances in Water Resources*, 45, 76–85. doi:10.1016/j.advwatres.2012.03.023
- Wang, Z., *et al.*, 2012. Using Markov switching models to infer dry and rainy periods from telecommunication microwave link signals. *Atmospheric Measurement Techniques*, 5, 1847–1859. doi:10.5194/amt-5-1847-2012